

Aryldiazenido Complexes: Syntheses of Iridium Complexes with Doubly-Bent Aryldiazenido Ligands and X-ray Structure of $[\text{Cp}^*\text{Ir}(\text{PMe}_3)_2(p\text{-N}_2\text{C}_6\text{H}_4\text{OMe})][\text{BF}_4]$

Grace Chi-Young Kim, Raymond J. Batchelor, Xiaoqian Yan, Frederick W. B. Einstein, and Derek Sutton*

Department of Chemistry, Simon Fraser University, Burnaby, British Columbia, Canada V5A 1S6

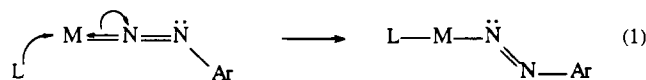
Received August 9, 1995*

$[\text{Cp}^*\text{Ir}(\text{C}_2\text{H}_4)(\text{N}_2\text{Ar})][\text{BF}_4]$ (**1**; Ar = *p*-C₆H₄OMe) reacts with PMe_3 to give $[\text{Cp}^*\text{Ir}(\text{PMe}_3)_2(\text{N}_2\text{Ar})][\text{BF}_4]$ (**4**), which has been shown by an X-ray structure determination and by ¹⁵N NMR spectroscopy to possess the aryldiazenido ligand bound with doubly-bent geometry. As is the case in **1**, the complexes $[\text{Cp}^*\text{Ir}(\text{PPh}_3)(\text{N}_2\text{Ar})][\text{BF}_4]$ (**2**) and $[\text{Cp}^*\text{Ir}\{\text{P}(p\text{-tol})_3\}(\text{N}_2\text{Ar})][\text{BF}_4]$ (**3**) have the N₂Ar ligand bound with singly-bent geometry. This has been demonstrated by an X-ray structure determination for **3**. Complexes **2** and **3** react with PMe_3 to give $[\text{Cp}^*\text{Ir}(\text{PPh}_3)(\text{PMe}_3)(\text{N}_2\text{Ar})][\text{BF}_4]$ (**5**) and $[\text{Cp}^*\text{Ir}\{\text{P}(p\text{-tol})_3\}(\text{PMe}_3)(\text{N}_2\text{Ar})][\text{BF}_4]$ (**6**), and **2** reacts with CO or CN⁻ to give $[\text{Cp}^*\text{Ir}(\text{CO})(\text{PPh}_3)(\text{N}_2\text{Ar})][\text{BF}_4]$ (**7**) or $\text{Cp}^*\text{Ir}(\text{CN})(\text{PPh}_3)(\text{N}_2\text{Ar})$ (**8**). All these reactions are shown by ¹⁵N NMR to involve the transformation of the N₂Ar ligand from singly-bent to doubly-bent as a consequence of coordination by the incoming ligand. Diphos (Ph₂P(CH₂)₂PPh₂) reacts with **1** to give $[\text{Cp}^*\text{Ir}(\text{diphos})(\text{N}_2\text{Ar})][\text{BF}_4]$ (**9**), but no complex of stoichiometry $[\text{Cp}^*\text{Ir}(\text{PPh}_3)_2(\text{N}_2\text{Ar})][\text{BF}_4]$ could be obtained from **1** or **2** with excess PPh₃; this complex is presumably sterically disfavored. Crystal structures: **3**, *T* = 295 K, orthorhombic, space group *P*2₁2₁2₁, *Z* = 4; *a* = 12.974(2) Å; *b* = 13.449(2) Å, *c* = 16.213(4) Å, *V* = 2829.0 Å³, *R*_F = 0.032 for 2974 data (*I*_o ≥ 2.5σ(*I*_o)) and 241 variables; **4**, *T* = 295 K, monoclinic, space group *P*2₁/*n*, *Z* = 4; *a* = 9.906(2) Å, *b* = 12.084(3) Å, *c* = 30.545(6) Å, β = 93.296(13)°, *V* = 3650.2 Å³, *R*_F = 0.029 for 3606 data (*I*_o ≥ 2.5σ(*I*_o)) and 422 variables.

Introduction

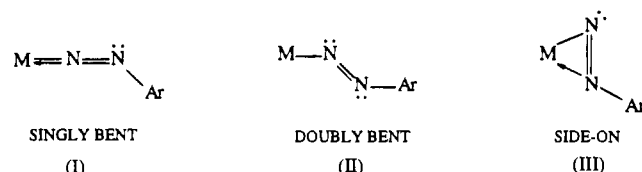
Over the last two decades, there has been considerable interest in the study of the aryldiazenido ligand (NNAr) in transition metal compounds with respect to its capability of adopting a wide range of coordination geometries.¹ In mononuclear aryldiazenido compounds, the N₂Ar ligand can bind to the metal in three different coordination modes, i.e., singly-bent (I), doubly-bent (II), and side-on (III) (Chart 1), depending on the metal and ancillary ligands.^{1–3}

One possible strategy for the synthesis of doubly-bent N₂Ar complexes (II) is the complexation of a 2-electron-donor ligand L to a singly-bent N₂Ar complex (I) as shown in eq 1.



Some 20 years ago, Haymore and Ibers showed that the five-coordinate Ru and Os complexes $[\text{M}(\text{CO})_2(\text{PPh}_3)_2(\text{N}_2\text{Ph})][\text{PF}_6]$, with singly-bent N₂Ph ligands, reacted with coordinating anions to yield six-coordinate complexes. These were considered to contain doubly-bent N₂Ar ligands on the basis of ν(NN) assignments in the IR spectra.⁴ To our knowledge, there have been no other reported examples of this type of reaction for aryldiazenido complexes.⁵ Recently, we observed that the singly-bent aryldiazenido complex $[\text{Cp}^*\text{Ir}(\text{PPh}_3)(\text{N}_2\text{Ar})][\text{BF}_4]$ (**2**, Ar = *p*-C₆H₄OMe, reacted with NaBH₄ to yield $\text{Cp}^*\text{IrH}(\text{PPh}_3)(\text{N}_2\text{Ar})$, which was assigned on the basis of ¹⁵N

Chart 1



NMR spectroscopy to contain a doubly-bent N₂Ar group.⁶ This appeared to be a new example of eq 1 and prompted us to examine additions of other potential ligands to **2** or its precursor, the ethylene complex **1**.

Experimental Section

All solvents were dried and purified by standard methods and were freshly distilled under nitrogen immediately before use. All reactions and manipulations were carried out in standard Schlenk ware, connected to a switchable double manifold providing vacuum and nitrogen. Reactions were performed at room temperature, unless otherwise mentioned. Infrared spectra were measured for solutions in CaF₂ cells by using a Bomem Michelson 120 FTIR instrument. Routine ¹H NMR spectra were recorded at 100 MHz by using a Bruker SY-100 Fourier transform spectrometer. Chemical shifts (δ) are reported in ppm, downfield positive, relative to tetramethylsilane (TMS). ¹⁵N NMR and ³¹P NMR spectra were obtained by Mrs. M. M. Tracey of the NMR service of Simon Fraser University on a Bruker AMX-400 Fourier transform instrument at operating frequencies of 40.5 and 162 MHz for ¹⁵N and ³¹P, respectively. Chemical shifts (ppm) are reported

* Abstract published in *Advance ACS Abstracts*, November 1, 1995.

(1) Johnson, B. F. G.; Haymore, B. L.; Dilworth, J. R. In *Comprehensive Coordination Chemistry*; Wilkinson, G., Gillard, R. D., McCleverty, J. A., Eds.; Pergamon Press: Oxford, England, 1987; Vol. 2, p 130.

(2) Sutton, D. *Chem. Rev.* **1993**, *93*, 995.

(3) Sutton, D. *Chem. Soc. Rev.* **1975**, *4*, 443.

(4) Haymore, B. L.; Ibers, J. A. *Inorg. Chem.* **1975**, *14*, 2784.

(5) (a) Linear (3e⁻) to bent (1e⁻) transformations of nitrosyl ligands by coordination of an additional 2e⁻-donor ligand are somewhat better established. See: Weiner, W. P.; Bergman, R. G. *J. Am. Chem. Soc.* **1983**, *105*, 3922. Enemark, J. H.; Feltham, R. D.; Huie, B. T.; Johnson, P. L.; Swedo, K. B. *J. Am. Chem. Soc.* **1977**, *99*, 3285. Enemark, J. H.; Feltham, R. D.; Riker-Nappier, J.; Bizot, K. F. *Inorg. Chem.* **1975**, *14*, 624. (b) We are indebted to a reviewer for pointing out that $[\text{IrCl}(\text{diphos})_2(\text{N}_2\text{Ar})]^+$ was synthesized by halide addition to $[\text{Ir}(\text{diphos})_2(\text{N}_2\text{Ar})]^{2+}$ (see refs 17 and 23).

(6) Yan, X.; Einstein, F. W. B.; Sutton, D. *Can. J. Chem.* **1995**, *73*, 939.

(downfield positive) with respect to the external references MeNO₂ for ¹⁵N and 85% H₃PO₄ for ³¹P. Fast atom bombardment (FAB) or electron impact (EI) mass spectra were obtained by Mr. G. Owen on a Hewlett-Packard Model 5985 spectrometer equipped with a fast atom bombardment probe (xenon source, Phrasor Scientific, Inc., accessory). Samples for FABMS were dissolved in *m*-nitrobenzyl alcohol (NOBA). The observed isotope patterns of the parent and fragment ions are reported on the basis of the more abundant isotope ¹⁹³Ir. Microanalyses were performed by Mr. M. K. Yang of the Microanalytical Laboratory of Simon Fraser University. The melting points were obtained by using a Fisher-Johns melting point apparatus and are uncorrected.

The *p*-methoxybenzenediazonium tetrafluoroborate was prepared by the standard procedure using *p*-anisidine (Aldrich) and sodium nitrite. It was recrystallized periodically from acetone and diethyl ether. The ¹⁵N_α-labeled salt [*p*-¹⁵NNC₆H₄OMe][BF₄] was prepared from Na¹⁵NO₂ (95% ¹⁵N enriched, MSD Isotopes) and was employed for the syntheses of ¹⁵N-labeled compounds. The syntheses of [Cp*Ir(C₂H₄)(*p*-N₂C₆H₄OMe)][BF₄] (1) and [Cp*Ir(PPh₃)(*p*-N₂C₆H₄OMe)][BF₄] (2) have been reported previously.^{6,7}

Preparation of [(η⁵-C₅Me₅)Ir{P(*p*-tol)₃}(*p*-N₂C₆H₄OMe)][BF₄] (3). Cp*Ir(C₂H₄)(*p*-N₂C₆H₄OMe)][BF₄] (1) (30 mg; 0.052 mmol) in acetone (5 mL) was stirred with equimolar P(*p*-tol)₃ (16 mg; 0.052 mmol) at 0 °C for 15 min. The reaction mixture immediately changed color from yellow to orange. Excess hexane was then added with stirring until no further precipitation occurred. Recrystallization from acetone/hexane (1:5) at -10 °C gave orange crystals suitable for X-ray crystal analysis (35 mg, 0.041 mmol, 79%). IR: ν(NN) 1709 cm⁻¹ (EtOH); ν(¹⁵NN) 1674 cm⁻¹ (EtOH). ¹H NMR (294 K, acetone-*d*₆): δ 2.04 (d, *J*_{P-H} = 2 Hz, 15H, Cp*), 2.35 (s, 9H, *p*-C₆H₄OMe), 3.86 (s, 3H, *p*-C₆H₄OMe), 6.94 (d, 2H, *p*-C₆H₄OMe), 7.10 (d, 2H, *p*-C₆H₄OMe), 7.23–7.42 (m, 12H, *p*-C₆H₄OMe). ³¹P{¹H} NMR (acetone-*d*₆): δ 7.48 (d, *J*_{P-¹⁵N_α} = 6 Hz, P(*p*-tol)₃). ¹⁵N NMR (acetone-*d*₆): δ 33.68 (d, *J*_{P-¹⁵N_α} = 6 Hz, ¹⁵N_α). FABMS (NOBA, xenon): *m/z* 767 (M⁺), 631 (M⁺ - N₂C₆H₄OMe, H), 461 (M⁺ - P(*p*-tol)₃, 2H). Anal. Calcd: C, 53.45; H, 5.09; N, 3.28. Found: C, 53.51; H, 5.38; N, 2.93. Mp: 120–125 °C dec.

Reaction of P(*p*-tol)₃ with [*p*-N₂C₆H₄OMe][BF₄]. Tri-*p*-tolylphosphine (5 mg; 0.016 mmol) in acetone-*d*₆ (3 mL) and equimolar [*p*-N₂C₆H₄OMe][BF₄] (3.7 mg; 0.016 mmol) were mixed and stirred for 5 min. The colorless solution immediately changed to orange. After workup, the resulting solid was identified by NMR as [(*p*-tol)₃P-N₂C₆H₄OMe][BF₄]. ¹H NMR (294 K, acetone-*d*₆): δ 2.54 (s, 9H, *p*-C₆H₄OMe), 4.03 (s, 3H, *p*-C₆H₄OMe), 7.26 (d, 2H, *p*-C₆H₄OMe), 8.15 (d, 2H, *p*-C₆H₄OMe), 7.59–7.90 (m, 12H, *p*-C₆H₄OMe).

Preparation of [(η⁵-C₅Me₅)Ir(PMe₃)₂(*p*-N₂C₆H₄OMe)][BF₄] (4). To an acetone solution (5 mL) containing [Cp*Ir(C₂H₄)(*p*-N₂C₆H₄OMe)][BF₄] (1) (30 mg; 0.052 mmol) was added by syringe a slight excess of PMe₃ in acetone. The solution immediately changed color from yellow to yellowish orange. The reaction mixture was stirred for 15 min. Excess hexane was then added with stirring in order to precipitate the orange solid. Recrystallization of 4 from acetone/hexane (1:5) at -10 °C gave reddish orange crystals (thin needles) suitable for X-ray analysis; yield 29 mg, 0.04 mmol, 80%. IR: ν(NN) 1466, ν(¹⁵NN) 1453 cm⁻¹ (CH₂Cl₂). ¹H NMR (acetone-*d*₆): δ 1.66 (d, *J*_{app} = 10 Hz, 18H, PMe₃), 1.86 (t, *J*_{P-H} = 2 Hz, 15H, Cp*), 3.82 (s, 3H, *p*-C₆H₄OMe), 6.98 (d, 2H, *p*-C₆H₄OMe), 7.40 (d, 2H, *p*-C₆H₄OMe). ³¹P{¹H} NMR (acetone-*d*₆): δ -37.73 (s, PMe₃). ¹⁵N NMR (acetone-*d*₆): δ 243.1 (s, ¹⁵N_α). FABMS (NOBA, xenon): *m/z* 615 (M⁺), 539 (M⁺ - PMe₃), 480 (M⁺ - N₂C₆H₄OMe), 463 (M⁺ - 2 PMe₃). Anal. Calcd: C, 39.37; H, 5.76; N, 3.99. Found: C, 39.24; H, 5.73; N, 3.97. Mp: 143–146 °C dec.

Preparation of [(η⁵-C₅Me₅)Ir(PPh₃)(PMe₃)(*p*-N₂C₆H₄OMe)][BF₄] (5). To [Cp*Ir(PPh₃)(*p*-N₂C₆H₄OMe)][BF₄] (2) (50 mg; 0.062 mmol) in ethanol (5 mL) was added by syringe a slight excess of PMe₃ in acetone. The reaction mixture was stirred (*ca.* 15 min) until the ν(NN) stretch from compound 2 disappeared as monitored by IR. The solution remained orange, and no obvious color change was observed throughout the reaction. Excess hexane was then added with stirring in order to precipitate the product. Recrystallization from acetone/hexane (1:5) at room temperature gave yellowish orange 5 in 94% yield (51 mg,

0.058 mmol). IR: ν(NN) 1466, ν(¹⁵NN) 1456 cm⁻¹ (CH₂Cl₂). ¹H NMR (294 K, acetone-*d*₆): δ 1.24 (d, *J*_{P-H} = 11 Hz, 9H, PMe₃), 1.47 (t, *J*_{P-H} = 3 Hz, 15H, Cp*), 3.84 (s, 3H, *p*-C₆H₄OMe), 7.00 (d, 2H, *p*-C₆H₄OMe), 7.39 (d, 2H, *p*-C₆H₄OMe), 7.45–7.82 (m, 15H, PPh₃). ³¹P{¹H} NMR (acetone-*d*₆): δ -3.31 (d, *J*_{P-P} = 21 Hz, PPh₃), -36.20 (d, *J*_{P-P} = 21 Hz, PMe₃). ¹⁵N NMR (acetone-*d*₆): δ 234.1 (s, ¹⁵N_α). FABMS (NOBA, xenon): *m/z* 801 (M⁺), 725 (M⁺ - PMe₃), 666 (M⁺ - N₂C₆H₄OMe), 539 (M⁺ - PPh₃). Anal. Calcd for 5: C, 51.40; H, 5.23; N, 3.16. Calcd for 5·H₂O: C, 50.38; H, 5.35; N, 3.09. Found: C, 50.44; H, 5.56; N, 3.06. Mp: 112–116 °C dec.

Preparation of [(η⁵-C₅Me₅)Ir{P(*p*-tol)₃}(PMe₃)(*p*-N₂C₆H₄OMe)][BF₄] (6). A 0.1 mL portion of prediluted PMe₃ in acetone was directly added to [(η⁵-C₅Me₅)Ir{P(*p*-tol)₃}(*p*-N₂C₆H₄OMe)][BF₄] (3) (40 mg; 0.047 mmol) to give a yellowish orange solution. The reaction mixture was stirred until ν(NN) at 1709 cm⁻¹ (EtOH) from compound 3 disappeared (as monitored by IR). Excess hexane was added to precipitate the crude product. Recrystallization from acetone/hexane (1:5) at room temperature gave an orange solid in 93% yield (41 mg, 0.044 mmol). ¹H NMR (294 K, acetone-*d*₆): δ 1.23 (d, *J*_{P-H} = 11 Hz, 9H, PMe₃), 1.46 (t, *J*_{P-H} = 2 Hz, 15H, Cp*), 2.39 (s, 9H, *p*-C₆H₄OMe), 3.84 (s, 3H, *p*-C₆H₄OMe), 7.02 (d, 2H, *p*-C₆H₄OMe), 7.25–7.46 (m, 2H, *p*-C₆H₄OMe), 7.25–7.46 (m, 12H, *p*-C₆H₄OMe). ³¹P{¹H} NMR (acetone-*d*₆): δ -5.39 (d, *J*_{P-P} = 23 Hz, P(*p*-tol)₃), δ -36.03 (d, *J*_{P-P} = 23 Hz, PMe₃). ¹⁵N NMR (acetone-*d*₆): δ 236.1 (s, ¹⁵N_α). FABMS (NOBA, xenon): *m/z* 708 (M⁺ - N₂C₆H₄OMe), 631 (M⁺ - N₂C₆H₄OMe, PMe₃), 539 (M⁺ - P(*p*-tol)₃). Anal. Calcd: C, 52.95; H, 5.65; N, 3.01. Found: C, 52.75; H, 5.96; N, 3.00. Mp: 125–128 °C dec.

Preparation of [(η⁵-C₅Me₅)Ir(CO)(PPh₃)(*p*-N₂C₆H₄OMe)][BF₄] (7). Carbon monoxide (CP grade) was bubbled briefly (2–3 min) through an ethanol solution (5 mL) of 2 (50 mg; 0.062 mmol). The reaction mixture was stirred for 30 min. A color change from orange to yellowish orange was observed. The reaction proceeded with the disappearance of ν(NN) bands at 1701 cm⁻¹ (EtOH) and concurrent production of a ν(CO) band at 2039 cm⁻¹ (EtOH). Excess hexane was added to precipitate the crude product. Recrystallization from ethanol/hexane (1:5) gave a yellowish orange powder (50 mg, 0.059 mmol, 95%). IR: ν(CO) 2039 cm⁻¹ (EtOH). ¹H NMR (294 K, acetone-*d*₆): 1.78 (d, *J*_{P-H} = 3 Hz, 15H, Cp*), 3.82 (s, 3H, *p*-C₆H₄OMe), 6.91 (d, 2H, *p*-C₆H₄OMe), 7.13 (d, 2H, *p*-C₆H₄OMe), 7.47–7.80 (m, 15H, PPh₃). ³¹P{¹H} NMR (acetone-*d*₆): δ 2.52 (s, PPh₃). ¹⁵N NMR (acetone-*d*₆): δ 200.3 (s, ¹⁵N_α). FABMS (NOBA, xenon): *m/z* 753 (M⁺), 725 (M⁺ - CO), 618 (M⁺ - N₂C₆H₄OMe). Anal. Calcd: C, 51.49; H, 4.45; N, 3.34. Found: C, 51.66; H, 4.57; N, 3.59. Mp: 122–126 °C dec.

Preparation of (η⁵-C₅Me₅)Ir(CN)(PPh₃)(*p*-N₂C₆H₄OMe) (8). After [Cp*Ir(PPh₃)(*p*-N₂C₆H₄OMe)][BF₄] (2) (50 mg; 0.062 mmol) was synthesized in ethanol (5 mL), excess KCN was added, and the mixture was stirred for 15 min. The orange solution slowly changed to yellowish orange and then slowly formed a yellowish orange precipitate. When no more solid precipitated, the mother liquid was removed and the remaining orange solid was vacuum-dried. The isolated solid exhibited low solubility in ethanol, acetone, hexane, and diethyl ether. IR: ν(CN) 2108 cm⁻¹ (EtOH). ¹H NMR (294 K, acetone-*d*₆): δ 1.48 (d, *J*_{P-H} = 2 Hz, 15H, Cp*), 3.75 (s, 3H, *p*-C₆H₄OMe), 6.81 (d, 4H, *p*-C₆H₄OMe), 7.30–7.77 (m, 15H, PPh₃). ³¹P{¹H} NMR (acetone-*d*₆): δ 6.99 (s, PPh₃). ¹⁵N NMR (acetone-*d*₆): δ 247.5 (s, ¹⁵N_α). EIMS: *m/z* 723 (M⁺ - CN, 2H), 590 (M⁺ - N₂C₆H₄OMe, CN, 2H).

Preparation of [(η⁵-C₅Me₅)Ir(Ph₂PC₂H₄PPH₂)(*p*-N₂C₆H₄OMe)][BF₄] (9). To [Cp*Ir(C₂H₄)(*p*-N₂C₆H₄OMe)][BF₄] (1) (30 mg; 0.052 mmol) in acetone (5 mL) was added an equimolar quantity of Ph₂PC₂H₄PPH₂ (diphos) (21 mg; 0.052 mmol), and the mixture was stirred for 15 min. An immediate color change from yellow to yellowish orange was observed. The loss of the ν(NN) absorption at 1724 cm⁻¹ in ethanol confirmed completion of the reaction. Excess hexane was added with stirring in order to precipitate the desired product. Recrystallization from acetone/hexane (1:5) at room temperature yielded a yellowish orange powder in 97% yield (48 mg, 0.050 mmol). ¹H NMR (294 K, acetone-*d*₆): 1.54 (t, *J*_{P-H} = 2 Hz, 15H, Cp*), 3.69 (s, 3H, *p*-C₆H₄OMe), 6.41 (d, 2H, *p*-C₆H₄OMe), 6.66 (d, 2H, *p*-C₆H₄OMe), 7.38–7.86 (m, 20 H, PPh₂). ³¹P{¹H} NMR (acetone-*d*₆): δ 43.84 (s, PPh₂). ¹⁵N NMR (acetone-*d*₆): δ 229.0 (s, ¹⁵N_α). FABMS (NOBA, xenon): *m/z* 726 (M⁺ - N₂C₆H₄OMe), 461 (M⁺ - diphos, 2H). Anal.

(7) Einstein, F. W. B.; Yan, X.; Sutton, D. J. *Chem. Soc., Chem. Commun.* 1990, 1466.

Table 1. Crystallographic Data for the Structure Determinations of [Cp*Ir{P(*p*-Tol)₃}(*p*-N₂C₆H₄OMe)][BF₄] (**3**) and [Cp*Ir(PMe₃)₂(*p*-N₂C₆H₄OMe)][BF₄] (**4**)

	3	4
formula	IrPF ₄ ON ₂ C ₃₈ BH ₄₃	IrP ₂ F ₄ ON ₂ C ₂₃ BH ₄₀
cryst syst	monoclinic	orthorhombic
fw	853.77	701.55
space group	P2 ₁ /n ^a	P2 ₁ 2 ₁ 2 ₁
<i>a</i> (Å) ^b	9.906(2)	12.974(2)
<i>b</i> (Å)	12.084(3)	13.449(2)
<i>c</i> (Å)	30.545(6)	16.213(4)
β (deg)	93.296(13)	
<i>V</i> (Å ³)	3650.2	2829.0
<i>Z</i>	4	4
ρ _c (g cm ⁻³)	1.554	1.647
λ(Mo Kα ₁) (Å)	0.709 30	0.709 30
μ(Mo Kα) (cm ⁻¹)	37.4	48.6
cryst dimens (mm)	0.25 × 0.26 × 0.35	0.30 × 0.35 × 0.35
transm factors ^c	0.398–0.512	0.316–0.411
2θ range	4–46	4–54
<i>R</i> _F ^d	0.029	0.032
<i>R</i> _{wF} ^e	0.035	0.039

^a The general equivalent positions for P2₁/n: *x*, *y*, *z*; $-x$, $-y$, $-z$; $1/2 + x$, $1/2 - y$, $1/2 + z$; $1/2 - x$, $1/2 + y$, $1/2 - z$. ^b Cell dimensions were determined in each case from 25 reflections (**3**, 36° ≤ 2θ ≤ 40°; **4**, 36° ≤ 2θ ≤ 41°). ^c The data were corrected by the Gaussian integration method for the effects of absorption. ^d $R_F = \sum(|F_o| - |F_c|) / \sum|F_o|$ for 3606 (**3**) and 2974 (**4**) data ($I_o \geq 2.5\sigma(I_o)$). ^e $R_{wF} = [\sum(w(|F_o| - |F_c|)^2) / \sum(wF_o^2)]^{1/2}$ for observed data (see footnote c; **3**, $w = [\sum(F_o)^2 + 0.0001F_o^2]^{-1}$; **4**, $w = [\sum(F_o)^2 + .0003F_o^2]^{-1}$).

Calcd: C, 54.48; H, 4.90; N, 2.96. Found: C, 54.56; H, 5.04; N, 2.70. Mp: 164–169 °C dec.

X-ray Structure Determinations for 3 and 4. Crystals were mounted in glass capillaries using a trace of Apiezon grease as an adhesive. The sample of **4** was cleaved from a larger crystal and mounted under dry nitrogen. Data were recorded at ambient temperature with an Enraf-Nonius CAD4F diffractometer using graphite-monochromatized Mo Kα radiation. All data were corrected for absorption by the Gaussian integration method, and calculated corrections for selected ψ-scanned reflections were carefully checked against the corresponding measured intensities. Data reduction also included corrections for Lorentz and polarization effects and for intensity scale variation (two standards measured every hour: **4**, total intensity decay = 16%; **3**, no significant intensity variations).

Hydrogen atoms were included in calculated positions (*d*(C–H) = 0.95 Å) with isotropic displacement parameters initially proportional to the equivalent isotropic displacement parameters for the carbon atoms to which they were bound. The hydrogen atoms were made to ride on their respective carbon atoms during refinement. Mean isotropic displacement parameters for groups of chemically equivalent hydrogen atoms were refined and the shifts applied to the individual hydrogen atom displacement parameters.

Weighting schemes based on counting statistics for which $\langle w(|F_o| - |F_c|)^2 \rangle$ was nearly constant as a function of both $|F_o|$ and $(\sin \theta)/\lambda$ were used. Computations were carried out on MicroVAX-II and 80486 computers. The programs used for absorption corrections, data reduction, structure solution, and graphical output were from the NRCVAX crystal structure system.⁸ Refinement was carried out using CRYSTALS.⁹ Complex scattering factors for neutral atoms¹⁰ were used in the calculation of structure factors. Crystallographic details are summarized in Table 1.

The structure of **4** was found to display extremely anisotropic thermal parameters for the Cp* ligand. It was finally modeled with two orientations, each as a rigid group, with a refined relative partial

Table 2. Fractional Coordinates and Isotropic or Equivalent Isotropic Displacement Parameters (Å²) for the Non-Hydrogen Atoms of [Cp*Ir(PMe₃)₂(*p*-N₂C₆H₄OMe)][BF₄] (**4**)

atom	<i>x</i>	<i>y</i>	<i>z</i>	<i>U</i> _{eq/iso} ^a
Ir	0.17897(2)	0.17852(2)	0.14228(2)	0.0447
P(1)	0.2617(2)	0.0280(2)	0.1400(2)	0.0553
P(2)	0.1783(2)	0.2011(2)	0.00230(13)	0.0537
O	-0.3790(5)	-0.1075(6)	0.0787(5)	0.0776
N(1)	0.0393(5)	0.1114(5)	0.1346(4)	0.0547
N(2)	0.0232(6)	0.0364(6)	0.0954(4)	0.0594
C(1)	0.2157(5)	0.2220(5)	0.2728(4)	0.065(3) ^b
C(2)	0.2861(4)	0.2708(5)	0.2215(4)	0.060(3) ^b
C(3)	0.2315(5)	0.3361(5)	0.1722(4)	0.062(3) ^b
C(4)	0.1269(4)	0.3277(5)	0.1912(4)	0.054(3) ^b
C(5)	0.1170(4)	0.2589(5)	0.2541(4)	0.053(3) ^b
C(11)	0.2440(8)	0.1527(7)	0.3461(6)	0.107(6) ^b
C(12)	0.4043(4)	0.2698(9)	0.2317(7)	0.099(6) ^b
C(13)	0.2792(7)	0.4182(7)	0.1172(6)	0.104(6) ^b
C(14)	0.0411(6)	0.4003(7)	0.1636(6)	0.096(5) ^b
C(15)	0.0152(5)	0.2300(8)	0.2969(6)	0.093(5) ^b
C(6)	0.2596(10)	0.2265(11)	0.2645(10)	0.065(3) ^c
C(7)	0.2868(9)	0.2966(12)	0.2049(10)	0.060(3) ^c
C(8)	0.1976(11)	0.3447(10)	0.1789(9)	0.062(3) ^c
C(9)	0.1141(9)	0.3024(11)	0.2195(9)	0.054(3) ^c
C(10)	0.1523(11)	0.2301(10)	0.2736(9)	0.053(3) ^c
C(16)	0.3355(15)	0.1741(18)	0.3244(15)	0.107(6) ^c
C(17)	0.3976(10)	0.3336(19)	0.1883(16)	0.099(6) ^c
C(18)	0.1947(18)	0.4438(14)	0.1299(14)	0.104(6) ^c
C(19)	0.0015(10)	0.3416(17)	0.2168(16)	0.096(5) ^c
C(20)	0.0869(16)	0.1672(16)	0.3348(13)	0.093(5) ^c
C(31)	0.2510(14)	-0.0560(10)	0.0514(10)	0.1050
C(32)	0.3992(8)	0.0279(9)	0.1532(12)	0.0962
C(33)	0.2153(14)	-0.0518(10)	0.2199(9)	0.1038
C(41)	0.1267(14)	0.1063(9)	-0.0671(7)	0.0908
C(42)	0.1006(9)	0.3052(9)	-0.0315(6)	0.0762
C(43)	0.3015(9)	0.2279(13)	-0.0441(7)	0.0906
C(21)	-0.0808(7)	-0.0009(6)	0.0950(5)	0.0534
C(22)	-0.1568(6)	0.0285(7)	0.1509(6)	0.0563
C(23)	-0.2557(7)	-0.0107(7)	0.1442(7)	0.0602
C(24)	-0.2781(7)	-0.0770(7)	0.0808(6)	0.0579
C(25)	-0.2033(8)	-0.1060(8)	0.0289(6)	0.0615
C(26)	-0.1033(8)	-0.0696(7)	0.0359(6)	0.0628
C(27)	-0.4121(9)	-0.1671(1)	0.0121(7)	0.0837
F(1)	0.2474(6)	0.6674(8)	0.1761(5)	0.1115
F(2)	0.3853(7)	0.7543(6)	0.1375(5)	0.1101
F(3)	0.4028(7)	0.6071(6)	0.1992(6)	0.1131
F(4)	0.3483(8)	0.7384(7)	0.2698(4)	0.1148
B(1)	0.3460(9)	0.691(1)	0.1959(8)	0.069(3)

^a The equivalent isotropic displacement parameter is the cube root of the product of the principal axes of the anisotropic displacement ellipsoid. ^b Occupancy = 0.698(7). ^c Occupancy = 1 - 0.698(7) = 0.302.

occupancy. An isotropic displacement parameter was refined for each disordered pair of carbon atoms. All other non-hydrogen atoms were allowed anisotropic displacement parameters, with the exception of the boron atom. The final full matrix least-squares refinement of 241 parameters (including an extinction parameter¹¹ of 0.25(5) μm) for 2974 observations converged (maximum |shift/esd| = 0.04) at *R* = 0.032. The maximum peak in the final difference map (0.8(1) e Å⁻³) occurred 0.11 Å from Ir. Final fractional coordinates for the non-hydrogen atom sites of **4** are listed in Table 2.

The absolute configuration for the crystal of **4** was established by measuring the intensities for all eight Laue-equivalent reflections for a list of 22 sets of indices which were predicted from the refined structure to show the most significant differences (ranging from 66σ(*F_o*) to 22σ(*F_o*)) between Friedel-related pairs of structure factors. After absorption corrections and data reduction, every case showed the same sign and approximate magnitude for ($|F_o^+| - |F_o^-|$) as for ($|F_c^+| - |F_c^-|$).

The structure of **3** was allowed anisotropic displacement parameters for all non-hydrogen atoms. The only disorder detected was in the conformation of the methyl groups of the *p*-tolylphosphine ligand as evidenced in contoured electron density difference maps. Six 0.5-

- (8) Gabe, E. J.; LePage, Y.; Charland, J.-P.; Lee, F. L.; White, P. S. NRCVAX—An Interactive Program System for Structure Analysis. *J. Appl. Crystallogr.* **1989**, *22*, 384.
 (9) Watkin, D. J.; Carruthers, J. R.; Betteridge, P. W. *CRYSTALS*; Chemical Crystallography Laboratory, University of Oxford: Oxford, England, 1984.
 (10) *International Tables for X-ray Crystallography*; Kynoch Press: Birmingham, England, 1975; Vol. IV, p 99.

- (11) Larson, A. C. in *Crystallographic Computing*, Ahmed F. R. Ed., Munksgaard, Copenhagen, 1970; p 291.

Table 3. Fractional Coordinates and Isotropic or Equivalent Isotropic Displacement Parameters (\AA^2) for the Non-Hydrogen Atoms of $[\text{Cp}^*\text{Ir}\{\text{P}(p\text{-tol}_3)\}_3\{p\text{-N}_2\text{C}_6\text{H}_4\text{OMe}\}][\text{BF}_4^-]$ (**3**)

atom	x	y	z	U_{eq}^a
Ir	0.00404(3)	0.09377(2)	0.14677(9)	0.0409
P	0.1830(2)	0.1483(2)	0.10589(7)	0.0449
O	-0.3426(7)	0.5181(6)	-0.0011(2)	0.0829
N(1)	-0.1034(6)	0.1009(5)	0.0968(2)	0.0494
N(2)	-0.1722(6)	0.1087(5)	0.0632(2)	0.0554
C(1)	-0.1133(8)	0.1242(6)	0.2057(2)	0.0502
C(2)	-0.1035(8)	0.0085(6)	0.1987(3)	0.0522
C(3)	0.0337(8)	-0.0247(6)	0.2039(2)	0.0489
C(4)	0.1116(8)	0.0719(6)	0.2120(2)	0.0500
C(5)	0.0208(8)	0.1646(6)	0.2138(2)	0.0513
C(11)	-0.2394(9)	0.1916(8)	0.2070(3)	0.0766
C(12)	-0.2226(9)	-0.0700(7)	0.1903(3)	0.0764
C(13)	0.0839(10)	-0.1418(7)	0.2051(3)	0.0694
C(14)	0.2618(8)	0.0763(8)	0.2236(3)	0.0734
C(15)	0.0578(10)	0.2791(7)	0.2294(3)	0.0680
C(21)	-0.2239(7)	0.2147(7)	0.0489(2)	0.0475
C(22)	-0.2150(8)	0.3113(7)	0.0744(3)	0.0593
C(23)	-0.2561(8)	0.4099(7)	0.0573(3)	0.0620
C(24)	-0.3071(8)	0.4151(8)	0.0135(3)	0.0627
C(25)	-0.3186(8)	0.3203(9)	-0.0114(3)	0.0687
C(26)	-0.2786(8)	0.2206(8)	0.0064(3)	0.0597
C(27)	-0.3847(11)	0.5277(10)	-0.0467(3)	0.0869
C(31)	0.1324(7)	0.1922(6)	0.0499(2)	0.0450
C(32)	0.1022(8)	0.3014(6)	0.0387(3)	0.0567
C(33)	0.0587(9)	0.3288(7)	-0.0037(3)	0.0683
C(34)	0.0402(8)	0.2512(7)	-0.0356(3)	0.0553
C(35)	0.0679(8)	0.1433(7)	-0.0249(3)	0.0620
C(36)	0.1142(8)	0.1133(6)	0.0170(3)	0.0566
C(37)	-0.0110(10)	0.2831(9)	-0.0813(3)	0.0868
C(41)	0.2722(7)	0.2662(6)	0.1297(2)	0.0428
C(42)	0.1966(8)	0.3597(6)	0.1404(2)	0.0486
C(43)	0.2591(9)	0.4556(7)	0.1556(3)	0.0564
C(44)	0.3984(8)	0.4627(7)	0.1616(3)	0.0551
C(45)	0.4727(8)	0.3703(7)	0.1530(3)	0.0572
C(46)	0.4134(8)	0.2733(7)	0.1370(3)	0.0587
C(47)	0.4647(10)	0.5691(7)	0.1758(3)	0.0746
C(51)	0.3118(7)	0.0440(6)	0.093(2)	0.0451
C(52)	0.3078(8)	-0.0559(7)	0.1169(3)	0.0569
C(53)	0.4044(8)	-0.1370(7)	0.1114(3)	0.0620
C(54)	0.5103(8)	-0.1181(7)	0.0853(3)	0.0610
C(55)	0.5127(8)	-0.0165(7)	0.0634(3)	0.0615
C(56)	0.4159(8)	0.0638(6)	0.0687(3)	0.0554
C(57)	0.6188(9)	-0.2029(8)	0.0789(3)	0.0863
F(1)	0.9785(10)	0.5832(8)	0.1999(4)	0.1814
F(2)	0.7971(7)	0.6388(6)	0.1661(3)	0.1303
F(3)	0.8967(10)	0.4827(7)	0.1508(2)	0.1553
F(4)	0.7921(10)	0.4941(7)	0.2067(3)	0.1592
B	0.8686(15)	0.5549(10)	0.1809(5)	0.0779

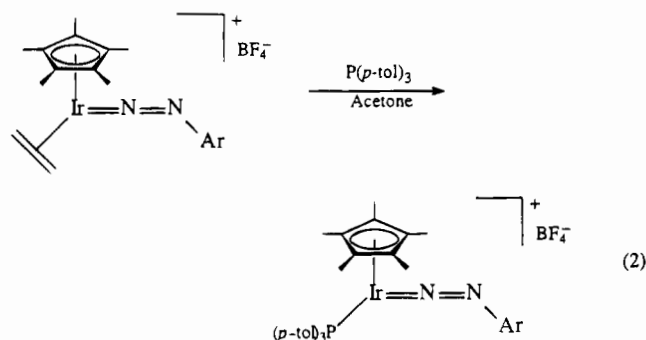
^a The equivalent isotropic displacement parameter is the cube root of the product of the principal axes of the anisotropic displacement ellipsoid.

occupied sites for the hydrogen atoms of each of these methyl groups were calculated for mutually staggered CH_3 conformations. The coordinates and displacement parameters for all hydrogen atoms were otherwise treated as described for **4**.

The final full-matrix least-squares refinement of 442 parameters for 3606 observations converged (maximum $|\text{shift}/\text{esd}| = 0.01$) at $R = 0.029$. The maximum peak in the final difference map ($0.7(1) \text{ e}\text{\AA}^{-3}$) occurred 1.05 \AA from Ir. Final fractional coordinates for the non-hydrogen atomic sites of **3** are listed in Table 3.

Results

Synthesis and Characterization of $[\text{Cp}^*\text{Ir}\{\text{P}(p\text{-tol}_3)\}_3\{p\text{-N}_2\text{C}_6\text{H}_4\text{OMe}\}][\text{BF}_4^-]$ (3**).** The new singly-bent aryldiazenido compound $[\text{Cp}^*\text{Ir}\{\text{P}(p\text{-tol}_3)\}_3\{p\text{-N}_2\text{C}_6\text{H}_4\text{OMe}\}][\text{BF}_4^-]$ (**3**) was isolated as an orange powder when $[\text{Cp}^*\text{Ir}(\text{C}_2\text{H}_4)\{p\text{-N}_2\text{C}_6\text{H}_4\text{OMe}\}][\text{BF}_4^-]$ (**1**) was treated with equimolar $\text{P}(p\text{-tol}_3)_3$ in acetone at 0°C (eq 2). Recrystallization from acetone/hexane gave orange crystals suitable for X-ray crystal analysis.



It should be noted that introducing an exact stoichiometric amount of $\text{P}(p\text{-tol}_3)_3$ is crucial to successfully synthesizing **3**. Addition of more than 1 equiv of $\text{P}(p\text{-tol}_3)_3$ resulted in a brown product, which according to ^1H NMR analysis contained many impurities. Furthermore, when compound **3** was synthesized by introducing $\text{P}(p\text{-tol}_3)_3$ and an aryldiazonium salt to $\text{Cp}^*\text{Ir}(\text{C}_2\text{H}_4)_2$ (the method favored for the synthesis of $[\text{Cp}^*\text{Ir}(\text{PPh}_3)\{p\text{-N}_2\text{C}_6\text{H}_4\text{OMe}\}]^+$),⁶ a byproduct identified as the adduct $[(p\text{-tol}_3)_3\text{P}\cdot p\text{-N}_2\text{C}_6\text{H}_4\text{OMe}][\text{BF}_4^-]$ was invariably observed in the ^1H NMR spectrum. The identity of this adduct was established by synthesizing it from $\text{P}(p\text{-tol}_3)_3$ and $[p\text{-N}_2\text{C}_6\text{H}_4\text{OMe}][\text{BF}_4^-]$ and comparing the ^1H NMR spectra. Similar adducts have been obtained by us previously.^{12,13}

Upon substituting the C_2H_4 ligand by $\text{P}(p\text{-tol}_3)_3$, we observed a new $\nu(\text{NN})$ band in the IR spectrum at 1709 cm^{-1} (EtOH). This falls within the typical range for the terminally coordinated singly-bent aryldiazenido ligand. A $^{15}\text{N}_\alpha$ -enriched sample showed an isotopic shift of 35 cm^{-1} .

In the ^1H NMR spectrum of **3**, $\text{P}(p\text{-tol}_3)_3$ coordination is indicated by a broad singlet at $\delta 2.35$ (integral 9H), corresponding to the $\text{P}(p\text{-tol}_3)_3$ methyl groups. The broadness of the resonance may be an indication that the $\text{P}(p\text{-tol}_3)_3$ ligand is nonrigid. Arylphosphorus ligands have often been observed to exhibit hindered rotation about the metal-phosphorus bond.¹⁴⁻¹⁶ However, in a variable-temperature ^1H NMR study of **3**, the resonance at $\delta 2.35$ showed no change upon cooling to -90°C . The Cp^* methyl resonance appeared as a doublet resulting from coupling to the single phosphorus nucleus. The singly-bent coordination mode of the aryldiazenido ligand in **3** was unambiguously demonstrated by the $^{15}\text{N}_\alpha$ resonance at $\delta 33.68$, which is well within the region assigned to singly-bent aryldiazenido compounds.¹⁷ Notably, $^{31}\text{P}\text{-}^{15}\text{N}$ coupling [$J_{\text{P-}^{15}\text{N}} = 6 \text{ Hz}$] was observed in both the $^{31}\text{P}\{^1\text{H}\}$ and ^{15}N NMR spectra. A similar result was obtained for $[\text{Cp}^*\text{Ir}(\text{PPh}_3)\{p\text{-N}_2\text{C}_6\text{H}_4\text{OMe}\}][\text{BF}_4^-]$ (**2**) [$J_{\text{P-}^{15}\text{N}} = 7 \text{ Hz}$].⁶

The spectroscopic data characterizing **3** and the other following new aryldiazenido compounds in this work are summarized in Table 4.

Syntheses and Characterizations of Doubly-Bent Aryldiazenido Compounds of the Type $[(\eta^5\text{-C}_5\text{Me}_5)\text{Ir}(\text{L}_1)(\text{L}_2)\{p\text{-N}_2\text{C}_6\text{H}_4\text{OMe}\}][\text{BF}_4^-]$. Several new iridium doubly-bent aryldiazenido compounds were synthesized by introducing a stoichiometric amount of PR_3 ($\text{PR}_3 = \text{PMe}_3, \text{Ph}_2\text{PC}_2\text{H}_4\text{PPh}_2$),

(12) Carroll, J. A.; Fisher, D. R.; Rayner Canham, G. W.; Sutton, D. *Can. J. Chem.* **1974**, *52*, 1914.

(13) Einstein, F. W. B.; Sutton, D.; Vogel, P. L. *Can. J. Chem.* **1978**, *56*, 891.

(14) Brunner, H.; Hammer, B.; Kruger, C.; Angermund, K.; Bernal, I. *Organometallics* **1985**, *4*, 1063.

(15) Jones, W. D.; Feher, F. J. *Inorg. Chem.* **1984**, *23*, 2376.

(16) Hunter, G.; Weakley, T. J. R. *J. Chem. Soc., Dalton Trans.* **1987**, 1545.

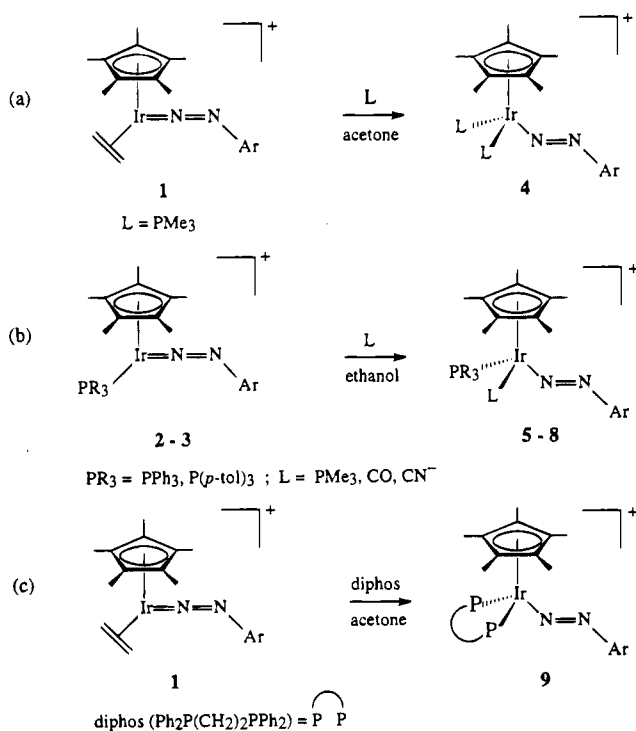
(17) Haymore, B. L.; Hughes, M.; Mason, J.; Raymond, R. L. *J. Chem. Soc., Dalton Trans.* **1988**, 2935.

Table 4. Summary of NMR Data for 1–9

complex ^{a,b}	$\delta(\text{Cp}^*)$ (ppm) ^c	¹⁵ N NMR (ppm) ^d	³¹ P{ ¹ H} NMR (ppm) ^e
[Cp*Ir(C ₂ H ₄)N ₂ Ar] ⁺ (1)	2.32 s	-2.26 s	
[Cp*Ir(PPh ₃)(N ₂ Ar)] ⁺ (2)	2.12 d	33.2 (d (² J _{P-¹⁵N} = 7 Hz))	9.57 d (² J _{P-¹⁵N} = 7 Hz)
[Cp*Ir{P(<i>p</i> -tol)} ₃](N ₂ Ar)] ⁺ (3)	2.04 d	33.7 d (² J _{P-¹⁵N} = 6 Hz)	7.20 d (² J _{P-¹⁵N} = 6 Hz)
[Cp*Ir(PMe ₃) ₂ (N ₂ Ar)] ⁺ (4)	1.86 t	243.1 s	-37.7 s
[Cp*Ir(PPh ₃)(PMe ₃)(N ₂ Ar)] ⁺ (5)	1.47 t	234.1 s	-3.31 d (² J _{P-P} = 13 Hz; PPh ₃) -36.2 d (² J _{P-P} = 13 Hz; PMe ₃)
[Cp*Ir{P(<i>p</i> -tol)} ₃](PMe ₃)(N ₂ Ar)] ⁺ (6)	1.46 t	236.1 s	-5.22 d (² J _{P-P} = 23 Hz; P(<i>p</i> -tol) ₃) -36.2 d (² J _{P-P} = 21 Hz; PMe ₃)
[Cp*Ir(PPh ₃)(CO)(N ₂ Ar)] ⁺ (7)	1.77 d	200.3 s	2.52 s
Cp*Ir(PPh ₃)(CN)(N ₂ Ar) (8)	1.48 d	247.5 s	6.99 s
[Cp*Ir(diphos)(N ₂ Ar)] ⁺ (9)	1.55 t	229.0 s	43.8 s

^a BF₄⁻ omitted; Ar = (*p*-C₆H₄OMe). ^b 1–3 are singly-bent aryldiazenido complexes; 4–9 are doubly-bent aryldiazenido complexes. ^c Measured in acetone-*d*₆ at room temperature. ^d Measured in acetone-*d*₆ referenced to external MeNO₂; ¹⁵N enriched at N_α only. ^e Measured in acetone-*d*₆ referenced to external 85% H₃PO₄; ¹⁵N_α-labeled sample used.

Scheme 1. Syntheses of Doubly Bent Aryldiazenido Complexes 4–9^a



^a BF₄⁻ anions omitted; Ar = *p*-C₆H₄OMe; 2 (R = Ph); 3 (R = *p*-tolyl); 4 (L = PMe₃); 5 (L = PMe₃, R = Ph); 6 (L = PMe₃, R = *p*-tolyl); 7 (L = CO, R = Ph); 8 (L = CN⁻, R = Ph).

CO, or CN⁻ to a solution of the singly-bent aryldiazenido compounds [Cp*Ir(PR₃)(*p*-N₂C₆H₄OMe)] [BF₄] [PR₃ = PPh₃ (2), P(*p*-tol)₃ (3)] or to their precursor [Cp*Ir(C₂H₄)(*p*-N₂C₆H₄OMe)] [BF₄] (1) (Scheme 1).

[Cp*Ir(PMe₃)₂(*p*-N₂C₆H₄OMe)] [BF₄] (4). When excess PMe₃ was added to [Cp*Ir(C₂H₄)(*p*-N₂C₆H₄OMe)] [BF₄] (1), instead of the expected mono(phosphine) complex with a singly-bent aryldiazenido ligand, *i.e.*, [Cp*Ir(PMe₃)(*p*-N₂C₆H₄OMe)] [BF₄], the bis(phosphine) complex [Cp*Ir(PMe₃)₂(*p*-N₂C₆H₄OMe)] [BF₄] (4) was isolated, implying that a doubly-bent aryldiazenido ligand had been formed (Scheme 1a). Recrystallization from acetone/hexane yielded reddish orange crystals suitable for X-ray crystal structure analysis.

The synthesis of 4 could not be monitored by IR for the possible formation of a mono(phosphine) intermediate since the solvent, acetone, shows strong absorption at ~1700 cm⁻¹, in the same region where $\nu(\text{NN})$ for a singly-bent N₂Ar ligand is expected. Substituting ethanol produced many impurities according to the ¹H NMR spectrum, and chlorinated solvents (*i.e.*,

CH₂Cl₂, CHCl₃) inevitably resulted in the formation of [Cp*Ir(PMe₃)Cl₂] identified by EIMS.

The presence of two PMe₃ groups in 4 was indicated by a virtual doublet proton resonance for PMe₃ at δ 1.66 with an integration of 18 H [*J*_{app} = 10 Hz]. A single sharp resonance at δ -37.73 in the ³¹P{¹H} NMR spectrum is consistent with the coordination of two *chemically equivalent* phosphorus ligands, and a triplet resonance at δ 1.86 for the Cp* methyl protons also indicates coupling to two chemically identical phosphorus nuclei. Most instructively, the ¹⁵N NMR spectrum gave a single ¹⁵N_α resonance at δ 243.1, which is in the typical chemical shift range for a doubly-bent aryldiazenido ligand.¹⁷ Notable was the absence of observable ³¹P-¹⁵N coupling in either the ¹⁵N or ³¹P{¹H} NMR spectra.⁴

The FABMS spectrum of 4 gave a parent peak at *m/z* 615 for the cation, followed by peaks at *m/z* 539 and 480, which are consistent with the loss of two PMe₃ ligands sequentially. The X-ray crystal structure of 4 unambiguously confirmed the doubly-bent geometry of the aryldiazenido ligand.

[Cp*Ir(PPh₃)(PMe₃)(*p*-N₂C₆H₄OMe)] [BF₄] (5) and [Cp*Ir{P(*p*-tol)}₃](PMe₃)(*p*-N₂C₆H₄OMe)] [BF₄] (6). Treating either [Cp*Ir(PPh₃)(*p*-N₂C₆H₄OMe)] [BF₄] (2) or [Cp*Ir{P(*p*-tol)}₃](*p*-N₂C₆H₄OMe)] [BF₄] (3) with a slight excess of PMe₃ resulted in the further coordination of 1 equiv of PMe₃ to yield the compounds [Cp*Ir(PPh₃)(PMe₃)(*p*-N₂C₆H₄OMe)] [BF₄] (5) and [Cp*Ir{P(*p*-tol)}₃](PMe₃)(*p*-N₂C₆H₄OMe)] [BF₄] (6) (Scheme 1b). The syntheses of 5 and 6 were monitored by IR spectroscopy. The bands at 1701 and 1709 cm⁻¹ corresponding to $\nu(\text{NN})$ of the singly-bent aryldiazenido ligand in 2 and 3 disappeared, but no new bands that could be assigned to $\nu(\text{NN})$ in the usual region for singly-bent N₂Ar (1600–2100 cm⁻¹) were observed. For 5 a band at 1466 cm⁻¹ (CH₂Cl₂) [1456 cm⁻¹ for 5-¹⁵N_α] is assigned to $\nu(\text{NN})$ of the doubly-bent N₂Ar ligand, but the small isotopic shift indicates coupling with other vibrations.¹

The coordination of two phosphorus ligands in 5 and 6 is supported by an apparent triplet for the Cp* methyl resonances at δ 1.47 and 1.46, respectively, in the ¹H NMR spectra [*J*_{P-H} = 2 Hz]. The presence of two different phosphorus ligands in 5 and in 6 is evident from the two sharp doublets in each of the ³¹P{¹H} NMR spectra. The PPh₃ and PMe₃ resonances of 5 appeared at δ -3.31 and -36.20, respectively, and the P(*p*-tol)₃ and PMe₃ resonances of 6 at δ -5.39 and -36.03, respectively. The N_α chemical shifts of 5 and 6 in the ¹⁵N NMR spectra occurred at δ 234.1 and 236.1, again clearly indicating the doubly-bent nature of aryldiazenido ligands in each case.¹⁷

[Cp*Ir(CO)(PPh₃)(*p*-N₂C₆H₄OMe)] [BF₄] (7) and Cp*Ir(CN)(PPh₃)(*p*-N₂C₆H₄OMe) (8). Upon reaction of CO with 2, the IR spectrum showed the complete disappearance of the $\nu(\text{NN})$ band at 1701 cm⁻¹ (in EtOH) for 2 and a concurrent

growth of $\nu(\text{CO})$ at 2039 cm^{-1} for coordinated CO in **7** (Scheme 1b). The ^1H NMR spectrum of **7** showed a slight change in chemical shifts from those observed in **2**. The $^{31}\text{P}\{^1\text{H}\}$ NMR spectrum showed a resonance at δ 2.52 corresponding to coordinated PPh_3 . Finally, a single resonance at δ 200.3 in the ^{15}N NMR spectrum confirms the formation of a doubly-bent N_2Ar ligand geometry in **7**.

Cyanide ion was also reacted with **2**, yielding a yellowish orange precipitate, proposed to be $\text{Cp}^*\text{Ir}(\text{CN})(\text{PPh}_3)(p\text{-N}_2\text{C}_6\text{H}_4\text{-OME})$ (**8**) (Scheme 1b). Again, the ^1H NMR spectrum of **8** showed only a slight change in chemical shifts compared with the spectrum of **2** before cyanide addition. The $^{31}\text{P}\{^1\text{H}\}$ (δ 6.99) and $^{15}\text{N}_\alpha$ (δ 247.5) NMR spectra indicated the presence of coordinated PPh_3 and a doubly-bent N_2Ar ligand, respectively. Unfortunately, the isolated product had a very low solubility in commonly used solvents such as ethanol, acetone, hexane, or diethyl ether, and the inability to find a suitable solvent that would satisfactorily dissolve it interfered with the full characterization of the compound. For example, the concentration of the sample in acetone- d_6 was sufficient for ^1H , $^{31}\text{P}\{^1\text{H}\}$, and ^{15}N NMR (95% ^{15}N -enriched sample used) analysis, but not for a good-quality $^{13}\text{C}\{^1\text{H}\}$ NMR analysis. The spectrum obtained from a $^{13}\text{C}\{^1\text{H}\}$ NMR overnight run showed no observable resonance assignable to carbon of a coordinated CN in the expected region *ca.* δ 140–180.^{18,19} Also, many weak unassignable resonances different from the expected resonances were observed, suggesting substantial decomposition during the run. Only a limited amount of the sample **8** dissolved in ethanol, and the IR spectrum of this solution showed a weak band near 2108 cm^{-1} , assigned to $\nu(\text{CN})$. The EI mass spectrum did not give a parent peak, but a peak at m/z 723 is assigned to the loss of CN accompanied by 2H from Cp^* .²⁰ While the compound has not been completely characterized, the data are in accord with its expected identity as the neutral complex $\text{Cp}^*\text{Ir}(\text{CN})(\text{PPh}_3)(p\text{-N}_2\text{C}_6\text{H}_4\text{OME})$.

[Cp*Ir(diphos)(p-N₂C₆H₄OMe)][BF₄] (9). $[\text{Cp}^*\text{Ir}(\text{C}_2\text{H}_4)(p\text{-N}_2\text{C}_6\text{H}_4\text{OME})][\text{BF}_4]$ (**1**) was treated with the bidentate ligand $\text{Ph}_2\text{PC}_2\text{H}_4\text{PPh}_2$ (diphos) to yield the doubly-bent aryldiazenido compound **9** (Scheme 1c). A triplet resonance for the Cp^* methyl protons at δ 1.55 in the ^1H NMR spectrum and a single resonance at δ 43.84 in the $^{31}\text{P}\{^1\text{H}\}$ NMR spectrum both indicate the coordination of two chemically identical phosphorus atoms. The doubly-bent aryldiazenido ligand geometry in **9** is confirmed by the N_α resonance at δ 229.0 in the ^{15}N NMR spectrum.

X-ray Structure of $[\text{Cp}^*\text{Ir}\{\text{P}(p\text{-tol})_3\}(p\text{-N}_2\text{C}_6\text{H}_4\text{OME})][\text{BF}_4]$ (3). A perspective view of the cation of **3** and the atomic labeling scheme are shown in Figure 1a, and a view down the $\text{Ir}-\text{N}(1)-\text{N}(2)$ direction is presented in Figure 1b. Selected intramolecular distances and angles are given in Table 5.

The crystal structure of **3** consists of an assemblage of discrete cations, $[\text{Cp}^*\text{Ir}\{\text{P}(p\text{-tol})_3\}(p\text{-N}_2\text{C}_6\text{H}_4\text{OME})]^+$, and anions, $[\text{BF}_4]^-$. There are no chemically significant intermolecular contacts. The geometry of the cation can be described as either a "half-sandwich" or a "two-legged piano-stool" structure where N_2Ar and $\text{P}(p\text{-tol})_3$ ligands represent the "legs". The $\text{P}-\text{Ir}-\text{N}(1)$ bond angle is $87.9(2)^\circ$, and the $\text{Cp}^*-\text{Ir}-\text{N}(1)$ and $\text{Cp}^*-\text{Ir}-\text{P}$ bond angles are each 139.4 and 132.5° , where Cp^* here denotes the centroid of the C_5Me_5 ring. The Cp^* ligand is bonded to the

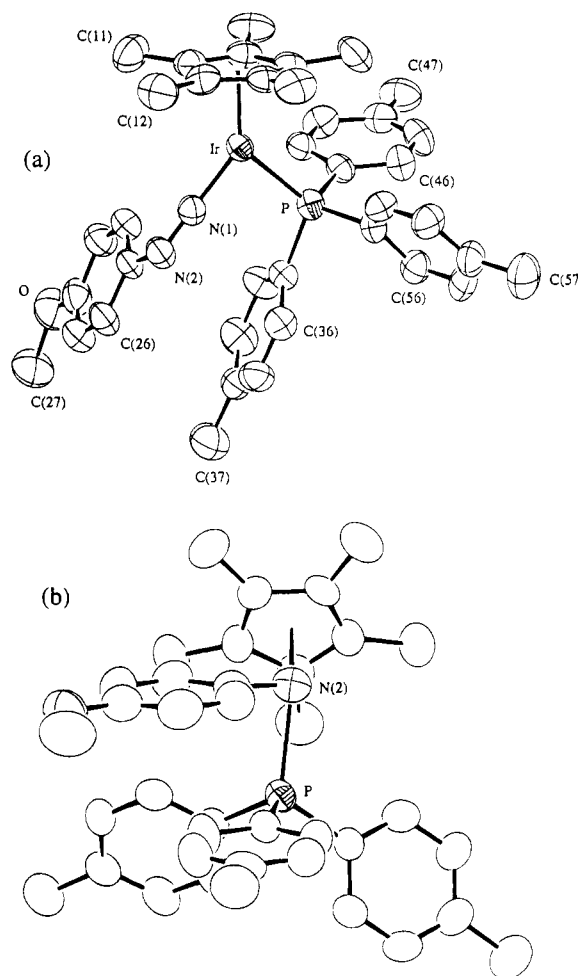


Figure 1. (a) Molecular structure of the complex cation of **3**. 50% probability displacement ellipsoids are shown for the non-hydrogen atoms. (b) View down the $\text{Ir}-\text{N}(1)-\text{N}(2)$ direction showing the orientation of the aryldiazenido ligand.

Table 5. Selected Intramolecular Distances (Å) and Angles (deg) for $[\text{Cp}^*\text{Ir}\{\text{P}(p\text{-tol})_3\}(p\text{-N}_2\text{C}_6\text{H}_4\text{OME})][\text{BF}_4]$ (**3**)

Distances			
$\text{Ir}-\text{P}$	2.322(2)	$\text{Ir}-\text{C}(3)$	2.263(7)
$\text{Ir}-\text{N}(1)$	1.811(6)	$\text{Ir}-\text{C}(4)$	2.221(7)
$\text{Ir}-\text{C}(1)$	2.228(7)	$\text{Ir}-\text{C}(5)$	2.215(8)
$\text{Ir}-\text{C}(2)$	2.215(7)	$\text{Ir}-\text{Cp}^a$	1.871
$\text{N}(1)-\text{N}(2)$	1.205(8)	$\text{N}(2)-\text{C}(21)$	1.437(12)
$\text{O}-\text{C}(24)$	1.361(12)	$\text{O}-\text{C}(27)$	1.435(12)
$\langle \text{P}-\text{C} \rangle$	1.821		
Angles			
$\text{P}-\text{Ir}-\text{Cp}$	132.5	$\text{N}(1)-\text{Ir}-\text{Cp}$	139.4
$\text{P}-\text{Ir}-\text{N}(1)$	87.9(2)	$\text{Ir}-\text{P}-\text{C}(51)$	116.3(2)
$\text{Ir}-\text{P}-\text{C}(31)$	114.0(2)	$\text{C}(31)-\text{P}-\text{C}(51)$	102.8(3)
$\text{Ir}-\text{P}-\text{C}(41)$	112.2(2)	$\text{C}(41)-\text{P}-\text{C}(51)$	105.9(3)
$\text{C}(31)-\text{P}-\text{C}(41)$	104.4(3)	$\text{N}(2)-\text{C}(21)-\text{C}(22)$	124.3(6)
$\text{Ir}-\text{N}(1)-\text{N}(2)$	177.7(6)	$\text{N}(2)-\text{C}(21)-\text{C}(26)$	116.4(7)
$\text{N}(1)-\text{N}(2)-\text{C}(21)$	120.2(7)		
$\text{P}-\text{C}(31)-\text{C}(32)$	123.3(6)	$\text{P}-\text{C}(41)-\text{C}(46)$	124.8(6)
$\text{P}-\text{C}(31)-\text{C}(36)$	119.5(6)	$\text{P}-\text{C}(51)-\text{C}(52)$	121.0(6)
$\text{P}-\text{C}(41)-\text{C}(42)$	118.2(5)	$\text{P}-\text{C}(51)-\text{C}(56)$	121.0(6)

^a Cp represents the center of mass of the five ring atoms of the Cp^* ligand.

iridium in the typical η^5 -coordination mode. The bond lengths from the five carbon atoms in the Cp^* ring to iridium range from 2.215(8) to 2.228(7) Å, with the exception of $\text{Ir}-\text{C}(3)$, which is 2.263(7) Å. The slight deviation in the $\text{Ir}-\text{C}(3)$ bond length can be attributed to the steric influence of the bulky $\text{P}(p\text{-tol})_3$ ligand. This ligand is pseudotrans to the aryldiazenido

- (18) Fujihara, T.; Kaizaki, S. *J. Chem. Soc., Dalton Trans.* **1993**, 1275.
 (19) Eller, S.; Schwarz, P.; Brimah, A. K.; Fischer, R. D. *Organometallics* **1993**, *12*, 3232.
 (20) Cp^* ligands have previously been observed to fragment by loss of 2H in Ir and Re compounds. See: Batchelor, R. J.; Einstein, F. W. B.; Lowe, N. D.; Palm, B. A.; Yan, X.; Sutton, D. *Organometallics* **1994**, *13*, 2041.

Table 6. Comparison of Distances (Å) and Angles (deg) for Iridium Singly-Bent Aryldiazenido Complexes

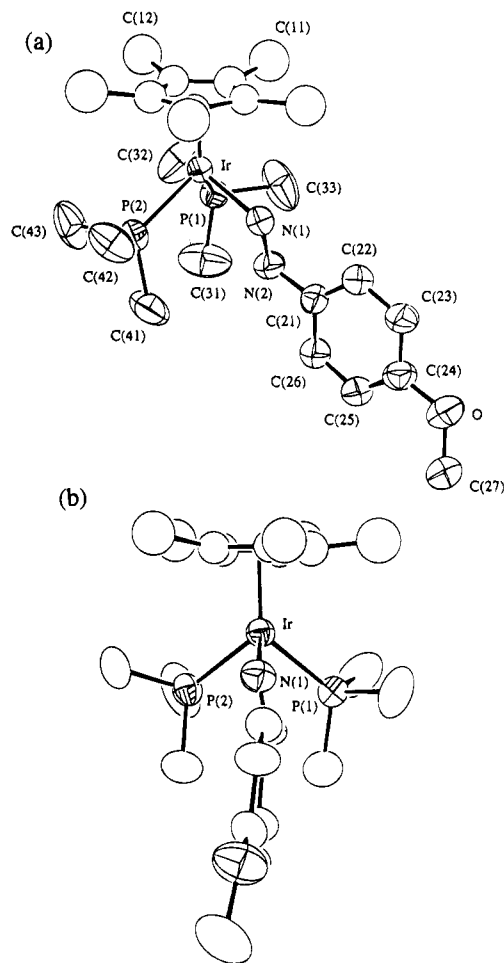
parameter	[Cp*Ir{P(<i>p</i> -tol) ₃ }- (N ₂ Ar)}] ⁺	[Cp*Ir(C ₂ H ₄)- (N ₂ Ar)}] ⁺ ^a	[IrCl(PPh ₃) ₂ - (N ₂ Ph)}] ⁺ ^b
Ir–N(1)	1.811(6)	1.811(7)	1.800(10)
N(1)–N(2)	1.205(8)	1.205(9)	1.163(11)
Ir–P	2.322(2)		2.350(2); 2.339(2)
Ir–N(1)–N(2)	177.7(6)	176.2(6)	175.8(8)
N(1)–N(2)–C(21)	120.2(7)	120.4(6)	126.9(10)

^a Reference 6. ^b Reference 21. ^c Ar = *p*-C₆H₄OMe.

ligand and is bound to Ir with an Ir–P bond length of 2.322(2) Å. The planes of the tolyl rings exhibit an interesting relationship with the surroundings. One eclipses the Ir–P bond and is the one with an ortho proton directed to C(3) of the Cp*⁺; the second is nearly parallel with the N₂Ar plane; and the third is nearly parallel with the Cp* plane. The aryldiazenido ligand clearly has a singly-bent geometry, in agreement with the values of $\nu(\text{NN})$ and the ¹⁵N_α chemical shift. The Ir–N(1)–N(2) and N(1)–N(2)–C(21) bond angles are respectively 177.7(6) and 120.2(7)°. The Ir–N(1) and N(1)–N(2) distances are 1.811(6) and 1.205(8) Å, which are in the range of values for previous structures of singly-bent aryldiazenido complexes of iridium (Table 6)^{6,21} and compare well with the dimensions in the singly-bent aryldiazenido complex [Cp*Ir(C₂H₄)(*p*-N₂C₆H₄OMe)][BF₄] (**1**).^{6,7} The projection view in Figure 1b illustrates that the N₂Ar plane is “horizontal”, i.e., perpendicular to the plane containing Ir, P, and the Cp* centroid. A comparable situation is also a feature of **1** and has been rationalized by simple molecular orbital arguments.⁶ The approximate planarity of the N₂Ar group [N(1)–N(2)–C(21)–C(22) and N(1)–N(2)–C(21)–C(26) torsion angles are –8.6(4) and 167.7(10)°, respectively] suggests near-optimal overlap of N(2) and phenyl ring π orbitals. Other torsion angles to note are Cp*–Ir–N(2)–C(21) 91.9°, C(27)–O–C(24)–C(25) –5.0(6)°, and N(1)–Ir–P–C(31) 9.2(3)°.

X-ray Structure of [Cp*Ir(PMe₃)₂(*p*-N₂C₆H₄OMe)][BF₄] (4**).** The structure consists of an assemblage of cations and anions with no chemically significant intermolecular contacts. A perspective view of the cation of **4** and the atomic labeling scheme are shown in Figure 2a. Selected intramolecular distances and angles are supplied in Table 7. The geometry of the cation of **4** can again be described as a “half-sandwich” or “piano-stool” structure but with three “legs”.

The PMe₃ ligands are related by an approximate mirror plane wherein lies the N₂Ar group (Figure 2b), and thus, as supported by the ¹H and ³¹P{¹H} NMR spectroscopic data, the two phosphorus ligands are situated in chemically identical environments with respect to the aryldiazenido ligand [Ir–P(1) = 2.292(2) Å; Ir–P(2) = 2.290(2) Å; P(1)–Ir–N(1) = 91.4(2)°; P(2)–Ir–N(2) = 89.7(2)°]. Of specific interest in the structure of **4** are the coordination mode and the orientation of the N₂Ar ligand. Unambiguously, the N₂Ar ligand has a doubly-bent geometry with Ir–N(1)–N(2) and N(1)–N(2)–C(21) bond angles of 123.9(6) and 117.1(8)°, respectively. The Ir–N(1) and N(1)–N(2) bond lengths of 2.028(7) and 1.210(10) Å are again as expected in comparison to those of other structurally determined doubly-bent aryldiazenido compounds (Table 8).^{22–24} The

**Figure 2.** Molecular structure of the complex cation of **4**. 50%-probability displacement ellipsoids for the non-hydrogen atoms are depicted. For clarity of presentation, only the major orientation of the disordered Cp* group is depicted. (b) View down the pseudo mirror plane that contains the aryldiazenido ligand.**Table 7.** Selected Intramolecular Distances (Å) and Angles (deg) for [Cp*Ir(PMe₃)₂(*p*-N₂C₆H₄OMe)][BF₄] (**4**)

Distances			
Ir–P(1)	2.292(2)	Ir–N(1)	2.028(7)
Ir–P(2)	2.290(2)	Ir–Cp ^a	1.94
⟨Ir–C⟩	2.275	⟨P–C⟩	1.81
N(1)–N(2)	1.210(10)	N(2)–C(21)	1.440(11)
Angles			
P(1)–Ir–P(2)	95.9(1)	⟨P(1)–Ir–Cp⟩	126
P(1)–Ir–N(1)	91.4(2)	⟨P(2)–Ir–Cp⟩	126
P(2)–Ir–N(1)	89.7(2)	⟨N(1)–Ir–Cp⟩	118
Ir–P(1)–C(31)	121.5(4)	Ir–P(2)–C(41)	121.3(4)
Ir–P(1)–C(32)	117.6(4)	Ir–P(2)–C(42)	113.9(4)
C(31)–P(1)–C(32)	99.7(8)	C(41)–P(2)–C(42)	98.6(6)
Ir–P(1)–C(33)	111.2(5)	Ir–P(2)–C(43)	115.9(4)
C(31)–P(1)–C(33)	99.9(7)	C(41)–P(2)–C(43)	102.0(8)
C(32)–P(1)–C(33)	104.4(9)	C(42)–P(2)–C(43)	102.2(6)
Ir–N(1)–N(2)	123.9(6)	N(1)–N(2)–C(21)	117.1(8)

^a Cp represents the occupancy-weighted center of mass of the ring carbon atoms of the disordered Cp* ligand.

stereochemistry about the N–N bond is trans, and the dihedral angle between the planes defined by the *p*-methoxyphenyl ring and by N(1)–N(2)–C(21) is 15°. The corresponding angles in other doubly-bent aryldiazenido complexes are comparable,

(25) Values of selected torsion angles in the structure of **4**: Cp–Ir–N(1)–N(2) –165.4°; Ir–N(1)–N(2)–C(21) –178.9(8)°; N(1)–N(2)–C(21)–C(22) –15.9(5)°; C(27)–O–C(24)–C(25) –6.5(7)°; N(1)–Ir–P(2)–C(43) –162.5(5)°.

(21) (a) Schramm, K. D.; Ibers, J. A. *J. Am. Chem. Soc.* **1978**, *100*, 2932.

(b) Schramm, K. D.; Ibers, J. A. *Inorg. Chem.* **1980**, *19*, 1231.

(22) Cobbledeick, R. E.; Einstein, F. W. B.; Farrell, N.; Gilchrist, A. B.; Sutton, D. J. *Chem. Soc., Dalton Trans.* **1977**, 373.

(23) (a) Gaughan, A. P.; Haymore, B. L.; Ibers, J. A.; Myers, W. H.; Nappier, T. E.; Meek, D. W. *J. Am. Chem. Soc.* **1973**, *95*, 6859. (b) Gaughan, A. P.; Haymore, B. L.; Ibers, J. A. *Inorg. Chem.* **1975**, *14*, 352.

(24) Krogsrud, S.; Ibers, J. A. *Inorg. Chem.* **1975**, *14*, 2298.

Table 8. Comparison of Distances (Å) and Angles (deg) for Doubly-Bent Aryldiazenido Complexes

complex	M–N	N–N	M–P	M–N–N	N–N–C
[Cp*Ir(PMe ₃) ₂ (N ₂ C ₆ H ₄ OMe)] ⁺ ^a	2.028(7)	1.210(10)	2.292(2); 2.290(2)	123.9(6)	117.1(8)
IrCl ₂ (CO)(PPh ₃) ₂ (<i>o</i> -N ₂ C ₆ H ₄ NO ₂) ^b	2.05(4)	1.19(4)	2.37(1)	115(3)	115(3)
PtCl(PEt ₃) ₂ (<i>p</i> -N ₂ C ₆ H ₄ F) ^c	1.97(3)	1.17(3)	2.302(4)	118(2)	118(2)
[RhCl(PPP)(N ₂ Ph)] ⁺ ^d	1.961(7)	1.172(9)	2.274(3)–2.368(3)	125.1(6)	118.9(8)

^a This work. ^b Reference 22. ^c Reference 24. ^d Reference 23.

ranging from 6 to 12°. The near-planarity of the aryldiazenido ligand again indicates extensive π conjugation including the *p*-methoxyphenyl ring and both nitrogens. Furthermore, compared with the situation in the singly-bent N₂Ar complexes **1** and **3** (Figure 1b), the plane containing the N₂Ar group is now rotated through 90° so as to lie “vertical” in the similarly oriented Newman projection viewed down the Ir–N(1) bond (Figure 2b). Now its plane essentially bisects the angle subtended at Ir by the two phosphorus groups. Such changes in the orientation of singly and doubly-bent N₂Ar ligands in complexes have been interpreted on the basis of simple MO theory.²⁶ What is perhaps most striking is a comparison of the structure of the cation of **4** with the structure of the rhenium complex of similar composition, *i.e.*, [Cp*Re(PMe₃)₂(*p*-N₂C₆H₄OMe)]⁺. In the latter, the N₂Ar group is *singly-bent* and is again oriented “horizontal”, *i.e.*, *perpendicular* to the plane equating the phosphine ligands.²⁷ This is only the fourth reported X-ray crystal structure of a complex containing a doubly-bent aryldiazenido ligand and the first for one with a “half-sandwich” type structure.

Discussion

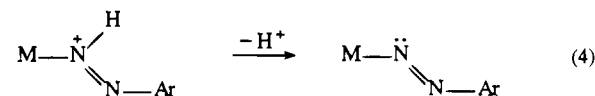
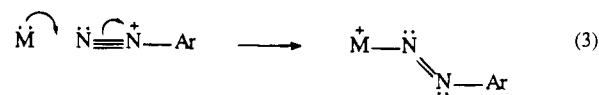
Doubly-bent aryldiazenido complexes date back to 1964, when Parshall first reported the platinum complexes PtCl(PEt₃)₂(*p*-N₂C₆H₄Y) (Y = F, H).^{28,29} In 1973, Haymore and Ibers³⁰ formulated IrCl(X)(L)(PPh₃)₂(*p*-N₂C₆H₄Y) (X = Cl, Br, I, N₃, NO₂, NCO; L = CO, EtNC; Y = F, H), and Robinson and co-workers^{31,32} similarly assigned the rhodium complexes RhX₂(PPh₃)₂(N₂Ar) to also possess doubly-bent aryldiazenido ligands. In the same year, Ibers and co-workers presented the first X-ray structure of a doubly-bent aryldiazenido complex, [RhCl(PPP)(N₂Ph)]⁺ [PPP = PhP{(CH₂)₃PPh₂}₂], and pointed out the potential unreliability of assigning singly-bent and doubly-bent aryldiazenido coordination modes solely on the basis of values of ν (NN) in the IR spectrum.²³ This complex showed relatively high values for ν (NN) (1627, 1561 cm⁻¹) that are well into the region usually assignable to singly-bent aryldiazenido compounds.

The X-ray structures of only two other doubly-bent aryldiazenido complexes have been reported: the Parshall complex PtCl(PEt₃)₂(*p*-N₂C₆H₄F)²⁴ and IrCl₂(CO)(PPh₃)₂(*o*-N₂C₆H₄NO₂),²² which confirmed the assignment of the complexes IrCl(X)(L)(PPh₃)₂(*p*-N₂C₆H₄Y) reported by Haymore and Ibers.³⁰ Other compounds such as [IrCl(diphos)₂(N₂Ph)]⁺,^{23a} [RhCl-

(diphos)₂(N₂Ph)]⁺,^{23a} and MX(CO)₂(PPh₃)₂(N₂Ph),^{4,23a} where M = Ru, Os, have been proposed to have doubly-bent aryldiazenido ligands.

Mason and co-workers have shown that the ¹⁵N NMR resonance of the N_α nitrogen provides a rather clear and easy way of distinguishing the coordination mode of the aryldiazenido ligand.^{17,33} For example, the ¹⁵N_α-labeled rhodium complexes RhCl₂(PPh₃)₂(*p*-N₂C₆H₄Y) exhibited N_α resonances which are shifted dramatically downfield (δ 327 for Y = NO₂; δ 298 for Y = H), by comparison with the N_α resonances of singly-bent aryldiazenido compounds which typically range from –28 to –56 ppm, and [IrBr(diphos)₂(N₂Ph)]⁺ and [RhCl(diphos)₂(N₂Ph)]⁺ displayed ¹⁵N_α resonances at δ 221 and 225, respectively.

Doubly-bent aryldiazenido complexes are much less abundant than singly-bent ones, and those that have been isolated to date result from (i) electrophilic attack or oxidative addition of N₂-Ar⁺ at an electron-rich metal center, sometimes with addition of an anionic ligand X⁻ (eq 3), (ii) deprotonation of the respective aryldiazeno compound (eq 4), or (iii) redistribution of electron density in an isolable singly-bent N₂Ar complex as a result of a coordination of an additional ligand (eq 1).



Several doubly-bent aryldiazenido compounds have been isolated by route i. For example, [Rh(PPP)Cl(N₂Ph)]⁺ was synthesized by oxidatively adding N₂Ph⁺ to Rh(PPP)Cl,^{23a} and IrCl₂(PPh₃)₂(CO)(N₂Ar) and RhX₂(PPh₃)₂(N₂Ar) were synthesized by reacting IrCl(CO)(PPh₃)₂ or RhX(PPh₃)₃ with the aryldiazonium salt in the presence of lithium halides.^{22,32} The complexes IrCl(X)(L)(PPh₃)₂(*p*-N₂C₆H₄Y) resulted from a similar procedure.³⁰ On the other hand, few doubly-bent aryldiazenido compounds have been synthesized by deprotonation of the respective aryldiazeno complex. Parshall synthesized PtCl(PEt₃)₂(N₂C₆H₅)²⁴ by deprotonating the phenyldiazeno complex [PtCl(PEt₃)₂(HNNPh)]⁺,³⁴ formed by reacting PtHCl(PEt₃)₂ with a diazonium salt.^{28,29} Similarly, MH(CO)₂(PPh₃)₂(N₂Ph) (M = Ru, Os) were also synthesized by deprotonating the respective aryldiazeno complexes [MH(CO)₂(PPh₃)₂(HNNPh)]⁺.⁴ While their formulation as doubly-bent N₂Ar complexes is probably correct, there are no published X-ray crystal structures or ¹⁵N NMR shifts to complement the IR data.

Prior to the present work, there appear to be few previous instances of route iii being used.^{5b} The singly-bent aryldiazenido complexes [Os(CO)₂(PPh₃)₂(N₂Ph)]⁺ and [Ru(CO)₂(PPh₃)₂(N₂Ph)]⁺ reacted with coordinating anions to yield six-coordinate complexes as mentioned above,⁴ and [Cp*Ir(PPh₃)(*p*-N₂C₆H₄OMe)][BF₄] reacted with H⁻ to form the doubly-bent aryldi-

(26) Yan, X. Ph.D. Thesis, Simon Fraser University, 1993; pp 25–29.

(27) Cusanelli, A.; Batchelor, R. J.; Einstein, F. W. B.; Sutton, D. *Organometallics* **1994**, *13*, 5096. The crystal structure determination was carried out on the carbonyl complex [Cp*Re(CO)(PMe₃)₂(*p*-N₂C₆H₄OMe)][BF₄], but variable-temperature NMR spectroscopy showed essentially similar limiting structures for this and the bis PMe₃ complex.

(28) Parshall, G. W. *J. Am. Chem. Soc.* **1965**, *87*, 2133.

(29) Parshall, G. W. *J. Am. Chem. Soc.* **1967**, *89*, 1822.

(30) Haymore, B. L.; Ibers, J. A. *J. Am. Chem. Soc.* **1973**, *95*, 3052.

(31) Laing, K. R.; Robinson, S. D.; Uttley, M. F. *J. Chem. Soc., Dalton Trans.* **1973**, 2713.

(32) (a) Laing, K. R.; Robinson, S. D.; Uttley, M. F. *J. Chem. Soc., Chem. Commun.* **1973**, 176. (b) Baird, M. C.; Wilkinson, G. *J. Chem. Soc. A* **1967**, 865.

(33) Dilworth, J. R.; Kan, C. T.; Richards, R. L.; Mason, J.; Stenhouse, I. *A. J. Organomet. Chem.* **1980**, *201*, C24.

(34) Ittel, S. D.; Ibers, J. A. *J. Am. Chem. Soc.* **1974**, *96*, 4804.

azenido compound $\text{Cp}^*\text{Ir}(\text{PPh}_3)\text{H}(p\text{-N}_2\text{C}_6\text{H}_4\text{OMe})$ identified as such by ^{15}N NMR [$\delta(^{15}\text{N}_\alpha)$ 272 ppm].⁶

In this work, the singly-bent aryldiazenido complex $[\text{Cp}^*\text{Ir}\{\text{P}(p\text{-tol})_3\}(p\text{-N}_2\text{C}_6\text{H}_4\text{OMe})][\text{BF}_4]$ (**3**) was isolated by substituting the ethylene group in $[\text{Cp}^*\text{Ir}(\text{C}_2\text{H}_4)(p\text{-N}_2\text{C}_6\text{H}_4\text{OMe})][\text{BF}_4]$ (**1**) with $\text{P}(p\text{-tol})_3$ as reported previously for **2**. This substitution occurs rather readily since the strong π back-bonding from Ir to the strong π acid (singly-bent aryldiazenido) ligand induces lability of the ethylene ligand. As observed for **2**, $\nu(\text{NN})$ of **3** occurs at a lower wavenumber than that exhibited by the starting complex $[\text{Cp}^*\text{Ir}(\text{C}_2\text{H}_4)(p\text{-N}_2\text{C}_6\text{H}_4\text{OMe})][\text{BF}_4]$ (**1**) (1709 cm^{-1} (**3**) vs 1724 cm^{-1} (**1**)). It was suggested that the better π acid character of the ethylene ligand in **1** compared with the phosphorus ligand in **2** provides less electron density at the metal center available for π back-bonding to the antibonding π orbitals of the aryldiazenido ligand, resulting in higher value of $\nu(\text{NN})$ for **1**.⁶ Similarly, the deshielded N_α chemical shift of δ 33.7 for **3** compared with δ -2.26 for **1** from the ^{15}N NMR spectra is thought to be essentially caused by an increase in π back-bonding. As mentioned elsewhere,⁶ compound **2** could also be synthesized by reacting PPh_3 and $[p\text{-N}_2\text{C}_6\text{H}_4\text{OMe}]^+$ with $[\text{Cp}^*\text{Ir}(\text{C}_2\text{H}_4)_2]$ directly. However, when this route was attempted for **3**, the adduct $[(p\text{-tol})_3\text{P}\cdot p\text{-N}_2\text{C}_6\text{H}_4\text{OMe}]^+$ was inevitably produced as a byproduct, as indicated by the separate synthesis of this adduct from $\text{P}(p\text{-tol})_3$ and $[p\text{-N}_2\text{C}_6\text{H}_4\text{OMe}]^+$ alone. This can be attributed to the difference in the basicity of the two triarylphosphines, and the more basic phosphorus atom center in $\text{P}(p\text{-tol})_3$ provides an alternative to the Ir metal center for electrophilic attack by $[p\text{-N}_2\text{C}_6\text{H}_4\text{OMe}]^+$. Reaction of an aryldiazonium ion with a phosphine has been observed previously. For example, the attempt to synthesize $[\text{Fe}(\text{CO})_2(\text{PPh}_3)_2(p\text{-N}_2\text{C}_6\text{H}_4\text{NEt}_2)]^+$ from $\text{Fe}(\text{CO})_3(\text{PPh}_3)_2$ and $[p\text{-N}_2\text{C}_6\text{H}_4\text{NEt}_2]^+$ resulted in a near-quantitative amount of $[\text{Ph}_3\text{P}\cdot p\text{-N}_2\text{C}_6\text{H}_4\text{NEt}_2]^+$.^{12,13}

While the reaction of $[\text{Cp}^*\text{Ir}(\text{C}_2\text{H}_4)(p\text{-N}_2\text{C}_6\text{H}_4\text{OMe})]^+$ with $\text{P}(p\text{-tol})_3$ yielded the expected singly-bent aryldiazenido complex **3**, 2 equiv of PMe_3 reacted to yield the doubly-bent aryldiazenido complex $[\text{Cp}^*\text{Ir}(\text{PMe}_3)_2(p\text{-N}_2\text{C}_6\text{H}_4\text{OMe})][\text{BF}_4]$ (**4**) (Scheme 1a). We presume that initially 1 equiv of PMe_3 coordinates first to form the singly-bent N_2Ar species $[\text{Cp}^*\text{Ir}(\text{PMe}_3)(p\text{-N}_2\text{C}_6\text{H}_4\text{OMe})]^+$, and sequential attack by another equivalent of PMe_3 results in the doubly-bent aryldiazenido compound **4**. The proposed intermediate $[\text{Cp}^*\text{Ir}(\text{PMe}_3)(p\text{-N}_2\text{C}_6\text{H}_4\text{OMe})]^+$ was not observed, presumably due to its more rapid reaction with a second equivalent of PMe_3 . Using less than an excess amount of PMe_3 lowered the rate of formation and yield of **4** significantly.

In order to substantiate this proposed mechanism, the reaction of PMe_3 , PPh_3 , or $\text{P}(p\text{-tol})_3$ with the singly-bent aryldiazenido compounds $[\text{Cp}^*\text{Ir}(\text{PPh}_3)(p\text{-N}_2\text{C}_6\text{H}_4\text{OMe})][\text{BF}_4]$ (**2**) and $[\text{Cp}^*\text{Ir}\{\text{P}(p\text{-tol})_3\}(p\text{-N}_2\text{C}_6\text{H}_4\text{OMe})][\text{BF}_4]$ (**3**) were investigated. PMe_3 coordinated to both **2** and **3**, yielding $[\text{Cp}^*\text{Ir}(\text{PPh}_3)(\text{PMe}_3)(p\text{-N}_2\text{C}_6\text{H}_4\text{OMe})][\text{BF}_4]$ (**5**) and $[\text{Cp}^*\text{Ir}\{\text{P}(p\text{-tol})_3\}(\text{PMe}_3)(p\text{-N}_2\text{C}_6\text{H}_4\text{OMe})][\text{BF}_4]$ (**6**) (Scheme 1b). The ^{15}N NMR of **5** and **6** clearly demonstrated isomerization of the singly-bent aryldiazenido ligand to the doubly-bent form to accommodate the addition of an additional electron pair donor to the metal (see below).

While 2 equiv of PMe_3 easily coordinated, forming the doubly-bent aryldiazenido complex $[\text{Cp}^*\text{Ir}(\text{PMe}_3)_2(p\text{-N}_2\text{C}_6\text{H}_4\text{OMe})][\text{BF}_4]$ (**4**), attempts to synthesize analogous bis(phosphine) compounds with 2 equivs of PPh_3 or of $\text{P}(p\text{-tol})_3$ did not succeed. Coordination of the bidentate ligand $\text{Ph}_2\text{PC}_2\text{H}_4\text{PPh}_2$ (diphos) to **1** was however successful and gave **9** (Scheme 1c). This suggests that the inability to synthesize $[\text{Cp}^*\text{Ir}(\text{PPh}_3)_2(p\text{-N}_2\text{C}_6\text{H}_4\text{OMe})]^+$ or $[\text{Cp}^*\text{Ir}\{\text{P}(p\text{-tol})_3\}_2(p\text{-N}_2\text{C}_6\text{H}_4\text{OMe})]^+$ probably is due

to steric hindrance, and the less sterically demanding diphos can coordinate both phosphorus atoms. As shown in Table 4, introducing a second ancillary ligand to the singly-bent aryldiazenido system causes more than a 200 ppm downfield chemical shift of the N_α resonance, clearly indicating the formation of a doubly-bent aryldiazenido ligand in the resulting complexes.^{17,33,35} Also observed is the disappearance of the $^{31}\text{P}\text{--}^{15}\text{N}$ coupling observed in the $^{31}\text{P}\{^1\text{H}\}$ and ^{15}N NMR spectra of the former. Thus, while $^{31}\text{P}\text{--}^{15}\text{N}$ coupling is easily observed in the singly-bent aryldiazenido complexes **2** and **3** [$J^{31}\text{P}\text{--}^{15}\text{N}$ = 6–7 Hz], where the phosphorus ligand and the N_2Ar ligand are pseudotrans to each other in a two-legged piano-stool structure, no measurable $^{31}\text{P}\text{--}^{15}\text{N}$ coupling is observed for the three-legged piano-stool, doubly-bent aryldiazenido complexes **4–9** that have the phosphorus groups in mutual cis positions. However, the $^{31}\text{P}\{^1\text{H}\}$ NMR spectra of **5** and **6** did clearly show $^{31}\text{P}\text{--}^{31}\text{P}$ coupling between the two inequivalent cis phosphorus ligands present. Some of the other reported doubly-bent aryldiazenido complexes, such as $[\text{Os}(\text{X})(\text{CO})_2(\text{PPh}_3)_2(\text{N}_2\text{Ph})]^+$ ⁴ and $\text{Cp}^*\text{Ir}(\text{H})(\text{PPh}_3)(p\text{-N}_2\text{C}_6\text{H}_4\text{OMe})$,⁶ have also displayed an absence of $^{31}\text{P}\text{--}^{15}\text{N}$ coupling in the $^{31}\text{P}\{^1\text{H}\}$ or ^{15}N NMR spectra.

Attempts were made to further establish the type of added ligand that is compatible with the doubly-bent aryldiazenido ligand in these complexes. This is because, while in this work coordination of weak π acid ligands, PR_3 , to the singly-bent aryldiazenido complex $[\text{Cp}^*\text{Ir}(\text{PPh}_3)(p\text{-N}_2\text{C}_6\text{H}_4\text{OMe})][\text{BF}_4]$ (**2**) was achieved easily under ambient conditions, previous attempts to coordinate hydride or a π basic ligand (Cl^-) had been shown to be less facile; *i.e.*, the synthesis of $\text{Cp}^*\text{Ir}(\text{PPh}_3)(\text{H})(p\text{-N}_2\text{C}_6\text{H}_4\text{OMe})$ required a low temperature, and the compound $\text{Cp}^*\text{Ir}(\text{PPh}_3)(\text{Cl})(p\text{-N}_2\text{C}_6\text{H}_4\text{OMe})$ could not be observed.⁶ Successful coordination of CO and CN^- ligands to **2**, if it occurred, might indicate that perhaps ligands with π acid character are preferred as the incoming ancillary ligand for stabilizing the doubly-bent aryldiazenido ligand in this system. Introducing CO and CN^- was observed to cause a dramatic downfield shift in the $^{15}\text{N}_\alpha$ resonance, strongly implying that coordination had occurred and that a doubly-bent N_2Ar group had resulted in **7** and **8** (Scheme 1b). For **7**, the IR spectrum showed $\nu(\text{CO})$ at 2039 cm^{-1} (EtOH). This is significantly lower than other reported $\nu(\text{CO})$ values (in the region of 2060 cm^{-1}) for the iridium(III) doubly-bent aryldiazenido complexes of general formula $\text{IrCl}_2(\text{CO})(\text{PPh}_3)_2(p\text{-N}_2\text{C}_6\text{H}_4\text{R})$ ($\text{R} = \text{H}, \text{F}, \text{Br}, \text{NO}_2, \text{OMe}$). Probably, the electron-donating Cp^* group in **7** provides the formal Ir(III) metal center with sufficient electron density to allow more $\pi \rightarrow \pi^*$ back-donation to the CO ligand, resulting in the low $\nu(\text{CO})$ value. The $\nu(\text{CN})$ value of 2108 cm^{-1} for **8** is in the expected region. Unfortunately, no other doubly-bent aryldiazenido complexes with cyano ligands exist for exact comparison.

While there have been many comparisons and discussions of the different bond distances and angles exhibited by the singly- and doubly-bent aryldiazenido ligands in their complexes, no particular attention has been paid to the difference in the orientation of the aryldiazenido ligands in these two geometries. In fact, such a difference was not readily apparent, since no related pairs of structurally determined singly- and doubly-bent aryldiazenido complexes in a comparable system existed previously. Only one indirect correlation has been made by comparing the singly-bent aryldiazenido compound $[(\eta^5\text{-C}_5\text{H}_4\text{CH}_3)\text{Mn}(\text{CO})_2(o\text{-N}_2\text{C}_6\text{H}_4\text{CF}_3)][\text{BF}_4]$ ³⁶ with the hydrazido-

(2-) compound $(\eta^5\text{-C}_5\text{H}_5)\text{Re}(\text{CO})_2\{\text{NN}(\text{Me})\text{C}_6\text{H}_4\text{OMe}\}$,³⁷ where it is proposed that, in order to establish a better overlap of the filled metal d orbital and the empty π^* orbital of the N_2Ar ligand, the transformation of a singly-bent to a doubly-bent aryldiazenido ligand is accompanied by a 90° ligand rotation about the $\text{M}-\text{N}_\alpha$ bond.²⁶ In this work, we now have obtained crystal structures of both singly- and doubly-bent aryldiazenido ligands in closely related complexes. As has been indicated above, a comparison of **3** and **4** confirms that the singly-bent to doubly-bent transformation is accompanied by a 90° ligand rotation about the metal- N_α bond.

Conclusion

In this work, one phosphorus ligand has been introduced into $[\text{Cp}^*\text{Ir}(\text{C}_2\text{H}_4)(p\text{-N}_2\text{C}_6\text{H}_4\text{OMe})]^+$ to yield a mono(phosphine) *singly-bent* aryldiazenido compound **3**. Subsequently, addition of two phosphorus ligands has been shown to be possible, to provide a series of bis(phosphine) *doubly-bent* aryldiazenido

compounds **4-6**. With the use of ^{15}N NMR spectroscopy, the systematic conversion of a singly-bent aryldiazenido compound to a doubly-bent aryldiazenido compound has been documented. More importantly, the crystal structures of a mono(phosphine) singly-bent and a bis(phosphine) doubly-bent aryldiazenido complex that share a similar overall geometry (*i.e.* piano-stool structure) have been determined, fully documenting the structural result of this transformation. Complexation of two phosphines results in the plane of the N_2Ar ligand rotating by 90° to lie perpendicular to the Cp^* plane.

Acknowledgment. This work was supported by the Natural Sciences and Engineering Council of Canada through research, equipment, and infrastructure grants to F.W.B.E. and D.S. The Johnson Matthey Co. is thanked for a generous loan of iridium trichloride.

Supporting Information Available: Listings of crystallographic experimental details, hydrogen positional and isotropic thermal parameters, anisotropic thermal parameters, bond distances, bond angles, and torsion angles (12 pages). Ordering information is given on any current masthead page.

- (36) (a) Barrientos-Penna, C. F.; Einstein, F. W. B.; Sutton, D.; Willis, A. C. *Inorg. Chem.* **1980**, *19*, 2740. (b) Barrientos-Penna, C. F.; Sutton, D. *J. Chem. Soc., Chem. Commun.* **1980**, 111.
(37) Barrientos-Penna, C. F.; Einstein, F. W. B.; Jones, T.; Sutton, D. *Inorg. Chem.* **1982**, *21*, 2578.

IC951045H